

Optimal rectification in the ultrastrong coupling regime

T. Werlang,* M. A. Marchiori, M. F. Cornelio, and D. Valente
Instituto de Física, Universidade Federal de Mato Grosso, Cuiabá MT, Brazil

(Received 3 April 2014; published 5 June 2014)

We study the effect of ultrastrong coupling on the transport of heat. In particular, we present a condition for optimal rectification, i.e., flow of heat in one direction and complete isolation in the opposite direction. We show that the strong-coupling formalism is necessary for correctly describing heat flow in a wide range of parameters, including moderate to low couplings. We present a situation in which the strong-coupling formalism predicts optimal rectification whereas the phenomenological approach predicts no heat flow in any direction, for the same parameter values.

DOI: [10.1103/PhysRevE.89.062109](https://doi.org/10.1103/PhysRevE.89.062109)

PACS number(s): 05.60.Gg, 03.65.Yz, 03.65.Ca

I. INTRODUCTION

Manipulation of individual quantum systems represents a breakthrough in the physical sciences [1]. It has been successfully achieved with single atoms [2,3], ions [4] or molecules [5], and more recently with artificial atoms, like quantum dots [6–10], or superconducting qubits [11,12]. It opens perspectives in quantum information processing, motivating studies on light-matter interaction at the single-photon level [13–17]. In analogy to modern electronic circuits, quantum devices have been proposed such as photon diodes [18,19] and photon transistors [20,21]. Diodes are current rectifiers. An optimal rectifier is able to conduct current in one sense and isolate it in the opposite sense.

All such realistic quantum systems are, of course, open. Natural atoms interact with electromagnetic environments [22]. Artificial atoms also interact with their solid-state environment. There is the need to understand, at the single-quantum level, for instance, the influence of temperature [23–25] and of phonons [26,27], fluctuating charges [28], and nuclear or electronic spins [29]. Analogies to diodes and transistors are also extendable to the flow of all such complex excitations [30].

Manipulation of individual quantum systems also gave birth to engineered interactions between those systems [31]. In particular, ultrastrong couplings are achieved, e.g., between a two-level system and a single-mode cavity in circuit quantum electrodynamics (QED) [32], totally modifying standard quantum optical scenarios [33].

In this paper, we explore heat transport under the influence of strong coupling between spins. We argue that the strong-coupling formalism is necessary even for moderate and low couplings. We treat a case where optimal rectification is expected within the strong-coupling description and is completely absent for the standard phenomenological approach. Optimal rectification is evidenced by the system of two spins coupled via Ising interaction. A broad range of experiments is capable of reproducing Ising-type interactions, simulating spins in the strong-coupling regime [34].

II. MODEL

The system of interest consists in a pair of interacting spins. We define the coupling constant Δ between the spins in the z direction. The magnetic field h applied to the spin on the left is also in the z direction. The Hamiltonian of the system is

$$H_S = \frac{\hbar}{2} \sigma_z^L + \frac{\Delta}{2} \sigma_z^L \sigma_z^R. \quad (1)$$

The spin on the left (right) is coupled with a thermal reservoir at a given temperature T_L (T_R). The system is illustrated in Fig. 1(a). The four eigenstates of H_S are given in terms of the eigenstates of $\sigma_z^{L(R)}$, $|\uparrow\rangle$, and $|\downarrow\rangle$, in decreasing energy order for the case of interest, $\Delta < h$, $|4\rangle = |\uparrow\uparrow\rangle$, $|3\rangle = |\uparrow\downarrow\rangle$, $|2\rangle = |\downarrow\downarrow\rangle$, $|1\rangle = |\downarrow\uparrow\rangle$. We define the transition frequencies as $\omega_{mn} = \epsilon_m - \epsilon_n$, where ϵ_k is the eigenvalue of H_S for the eigenstate $|k\rangle$. In the present case, they read $\omega_{41} = h + \Delta$, $\omega_{32} = h - \Delta$, $\omega_{43} = \omega_{21} = \Delta$, $\omega_{31} = \omega_{42} = h$.

The coupling to each bath of harmonic oscillators is given by the spin-boson model in the x component,

$$H_{\text{spin-res}}^{L(R)} = \sigma_x^{L(R)} \sum_k g_k (a_k^{L(R)} + a_k^{L(R)\dagger}), \quad (2)$$

with identical coupling strengths g_k . The Hamiltonians of the two free reservoirs are $H_{\text{res,L(R)}} = \sum_k \omega_k a_k^{L(R)\dagger} a_k^{L(R)}$. The model in Eq. (2) implies that the left (right) bath can only induce transitions on left (right) spin. Therefore, transitions $|4\rangle \leftrightarrow |2\rangle$ and $|3\rangle \leftrightarrow |1\rangle$, which simultaneously flip both spins, are forbidden. The rates at which the remaining transitions occur are computed in the following.

We derive a master equation to describe the system evolution. Here comes the crucial step for what follows: Strong-coupling formalism ($\Delta \sim h$) is employed [35]. This means that the Lindbladians are obtained on the basis of the eigenstates of the full system Hamiltonian H_S . Consequently, the dissipation mechanism of each spin depends not only on the coupling to its own bath but also on the coupling between the spins themselves. In a phenomenological approach, the Lindbladian derived for a single spin is joined to the master equation that describes the whole chain of spins as if each bath acted in a completely independent manner, disregarding the presence of other coupled spins. This is usually applied for extremely low couplings between the subsystems as compared to the transition frequency of the free subsystem, $\Delta \ll h$. An example is found in typical quantum optical scales, where

*thiago_werlang@fisica.ufmt.br

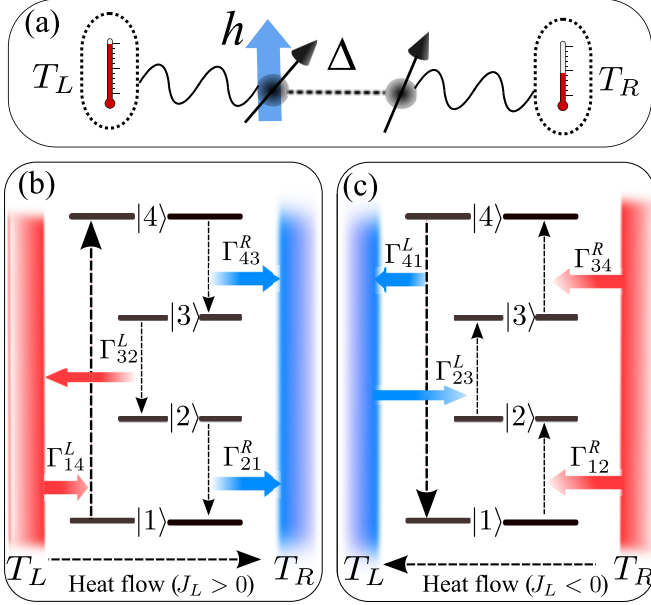


FIG. 1. (Color online) (a) Two spins coupled with strength Δ . Two independent thermal reservoirs are defined at temperatures T_L (T_R) for the bath on the left (right). (b) and (c) Case $\Delta < h$. $|1\rangle$ to $|4\rangle$ are the eigenstates of H_S in the corresponding case. (b) Energy transitions that allow for heat flow from the left hot bath to the right cold bath ($J_L > 0$, as defined in the text). $\Gamma_{ij}^{L(R)}$ is the net rate of transition from state $|i\rangle$ to $|j\rangle$, driven by the left (right) bath. The colored thick arrows indicate the flow of heat involved in each step of the cycle. (c) The same as (b) with reverted temperatures, and correspondingly reverted cycle. Note that in both cases the transition between states $|2\rangle$ and $|3\rangle$ involve heat exchange in the opposite sense with respect to the net heat flow. This is the key ingredient for the establishment of rectification, as explained in the text.

$\Delta/h \sim 10^{-11}-10^{-6}$ [1]. By contrast, the master equation derived here is valid even in the strong coupling regime. In the Born-Markov approximation with respect to the reservoirs, it reads [35]

$$\frac{d\rho}{dt} = -i[H_S, \rho] + \mathcal{L}_L[\rho] + \mathcal{L}_R[\rho], \quad (3)$$

in $\hbar = 1$ units, where the Lindblad operators $\mathcal{L}_{L(R)}[\rho]$ are given by

$$\begin{aligned} \mathcal{L}_{L(R)}[\rho] = & \sum_{\omega>0} \mathcal{J}(\omega) (1 + n_\omega^{L(R)}) \left[A_{L(R)}(\omega) \rho A_{L(R)}^\dagger(\omega) \right. \\ & \left. - \frac{1}{2} \{ \rho, A_{L(R)}^\dagger(\omega) A_{L(R)}(\omega) \} \right] \\ & + \mathcal{J}(\omega) n_\omega^{L(R)} \left[A_{L(R)}^\dagger(\omega) \rho A_{L(R)}(\omega) \right. \\ & \left. - \frac{1}{2} \{ \rho, A_{L(R)}(\omega) A_{L(R)}^\dagger(\omega) \} \right], \quad (4) \end{aligned}$$

where $\omega = \epsilon_j - \epsilon_i > 0$. The average number of excitations in each reservoir is given by the Bose-Einstein

distribution,

$$n_\omega^{L(R)} = \left[\exp \frac{\omega}{k_B T_{L(R)}} - 1 \right]^{-1},$$

and

$$A_{L(R)}(\omega) = \sum_{\omega=\epsilon_j-\epsilon_i} |i\rangle\langle i| \sigma_x^{L(R)} |j\rangle\langle j|$$

is the Lindblad operator associated with the transition driven by the bath from the left (right), with positive frequency ω . For $\Delta < h$, $\mathcal{L}_L[\rho]$ contains two nonvanishing operators, namely, $A_L(\omega_{41}) = |1\rangle\langle 4|$ and $A_L(\omega_{32}) = |2\rangle\langle 3|$, along with their adjoints. Because $\omega_{43} = \omega_{21}$, the only pair of nonvanishing operators for $\mathcal{L}_R[\rho]$ is $A_R(\omega_{43}) = |3\rangle\langle 4| + |1\rangle\langle 2|$ and $A_R^\dagger(\omega_{43})$. The baths are chosen to be ohmic, so the spectral functions are linear, $\mathcal{J}(\omega) = \kappa\omega$, where the constant κ is the same for both reservoirs.

III. DEFINITION OF THE HEAT CURRENT

Heat flow is characterized by heat current J_{heat} , defined with the aid of a continuity equation for the average energy going through the system $\langle H_S \rangle$ [23,24],

$$\frac{\partial}{\partial t} \langle H_S \rangle = -\nabla \cdot J_{\text{heat}} = -(J_R - J_L). \quad (5)$$

The left-hand side of Eq. (5), $\frac{\partial}{\partial t} \langle H_S \rangle = \frac{\partial}{\partial t} \text{Tr}\{\rho H_S\} = \text{Tr}\{\dot{\rho} H_S\}$, is calculated by the use of Eq. (3), providing

$$\frac{\partial}{\partial t} \langle H_S \rangle = \text{Tr}\{\mathcal{L}_L[\rho] H_S\} + \text{Tr}\{\mathcal{L}_R[\rho] H_S\}. \quad (6)$$

The rate of increase in the average energy of the system is then the sum of the input energy rate $J_{L(R)}^{\text{in}}$ from the left (right) reservoir,

$$J_{L(R)}^{\text{in}} \equiv \text{Tr}\{\mathcal{L}_{L(R)}[\rho] H_S\} = \pm J_{L(R)}. \quad (7)$$

IV. STEADY-STATE REGIME

We solve Eq. (3) in the steady-state regime, defined as $\dot{\rho}_{ss} = 0$, for which $\frac{\partial}{\partial t} \langle H_S \rangle = 0$, $J_L = -J_R$. In this case, the density matrix is diagonal in the energy eigenstates, $[H_S, \rho_{ss}] = 0$. So Eq. (3) reduces to

$$\dot{\rho}_{11} = 0 = \Gamma_{41}^L - \Gamma_{12}^R, \quad (8)$$

$$\dot{\rho}_{22} = 0 = -\Gamma_{23}^L + \Gamma_{12}^R, \quad (9)$$

$$\dot{\rho}_{33} = 0 = \Gamma_{23}^L - \Gamma_{34}^R, \quad (10)$$

$$\dot{\rho}_{44} = 0 = -\Gamma_{41}^L + \Gamma_{34}^R, \quad (11)$$

where

$$\Gamma_{ij}^{L(R)} \equiv \kappa \omega_{ij} [(1 + n_{\omega_{ij}}^{L(R)}) \rho_{ii} - n_{\omega_{ij}}^{L(R)} \rho_{jj}], \quad (12)$$

defined for $i > j$. The first term in the right-hand side of Eq. (12) is the decaying rate from state $|i\rangle$ to $|j\rangle$ and the second one is the excitation rate from $|j\rangle$ to $|i\rangle$. So $\Gamma_{ij}^{L(R)}$ is the net decaying rate from the state $|i\rangle$ to the state

$|j\rangle$. For $j > i$, $\Gamma_{ij}^{L(R)} = -\Gamma_{ji}^{L(R)}$ [see Figs. 1(b) and 1(c)]. System (8)–(11) shows that $\Gamma_{41}^L = \Gamma_{12}^R = \Gamma_{23}^L = \Gamma_{34}^R \equiv \Gamma$, that is, a single function Γ of the parameters Δ , h , and $T_{L(R)}$ governs the rate that the cycle runs (see Appendix A, Eqs. (A5) and (A6) for full expression of Γ). Figure 1(b) represents the case where $\Gamma < 0$, and Fig. 1(c), $\Gamma > 0$.

The steady-state current is computed,

$$J_L = -\omega_{41}\Gamma_{41}^L + \omega_{32}\Gamma_{23}^L = -2\Delta\Gamma,$$

where we have used that $\omega_{41} = h + \Delta$ and $\omega_{32} = h - \Delta$. In other words, the left bath absorbs from the left spin the amount ω_{41} of energy at rate $|\Gamma|$ and delivers ω_{32} of energy at the same rate, resulting in a net amount of 2Δ of exchanged energy per cycle. $J_L > 0$ is obtained when $-\Gamma > 0$, i.e., $-\Gamma = \Gamma_{14}^L > 0$. The last inequality means that energy leaves the left bath and goes to the left spin. Therefore, heat flows from the left to the right reservoir when $J_L > 0$ [Fig. 1(b)]. Heat current on the right spin is also computed, $J_R = \omega_{21}\Gamma_{12}^R + \omega_{43}\Gamma_{34}^R$. Using the definition of Γ and that $\omega_{41} = \omega_{43} + \omega_{32} + \omega_{21}$, we verify that $J_R = (\omega_{21} + \omega_{43})\Gamma = (\omega_{41} - \omega_{32})\Gamma = \omega_{41}\Gamma_{41}^L - \omega_{32}\Gamma_{23}^L = -J_L$, indeed.

V. RELEVANCE OF THE STRONG-COUPLING FORMALISM

We evidence the need for the use of strong-coupling formalism as far as an appropriate description of heat flow in a spin chain is concerned. In Fig. 2, J_L is shown as a function of T_L , at $T_R = 0$. We compare three regimes, namely, the strong-coupling regime $\Delta = 0.5h$ (blue, solid line), the moderate or intermediate regime $\Delta = 0.1h$ (red dashed line), and the low-coupling or weak regime $\Delta = 0.01h$ (black, dotted line). For all regimes, the current increases until saturating at a stationary value $J_L = \kappa\Delta^2/2$, since $\Gamma = -\kappa\Delta/4$ for $T_L \rightarrow \infty$

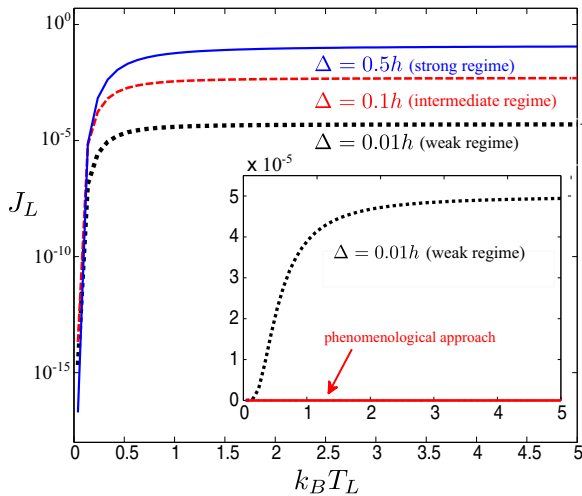


FIG. 2. (Color online) Left current J_L as a function of left bath temperature $k_B T_L$ for $T_R = 0$ and $\Delta = 0.01h$ (black dotted line, weak regime), $0.1h$ (red dashed line, intermediate regime), and $0.5h$ (blue solid line, strong regime). (Inset) Left current J_L from the microscopic approach (black dotted line) and the phenomenological approach (red solid line) as a function of $k_B T_L$ for $T_R = 0$ in the weak-coupling regime.

and $T_R \rightarrow 0$ (see Appendix A). Saturation in the energy flux is expected since the system has a finite number of energy levels.

The phenomenological model is obtained by replacing the Lindbladians operators in Eq. (3) by

$$\begin{aligned} \mathcal{L}_L^{ph}[\rho] = & \mathcal{J}(h)(1 + n_h^L) \left[\sigma_L^- \rho \sigma_L^- - \frac{1}{2} \{ \rho, \sigma_L^+ \sigma_L^- \} \right] \\ & + \mathcal{J}(h) n_h^L \left[\sigma_L^+ \rho \sigma_L^- - \frac{1}{2} \{ \rho, \sigma_L^- \sigma_L^+ \} \right], \end{aligned}$$

and $\mathcal{L}_R^{ph}[\rho]$, which is equal to the $\mathcal{L}_L^{ph}[\rho]$ with R instead of L and $h \rightarrow 0$. This model counterintuitively predicts zero heat current (see Appendix B), $J_L^{ph} = 0$, regardless of the temperature gradient, $T_L - T_R$, and of the coupling constant Δ . In the inset of Fig. 2, a comparison of the two approaches is made, particularly in the weak-coupling limit, $\Delta = 0.01h$ (red solid line for phenomenological, black dotted line for strong-coupling model).

In order to situate our results with respect to the pertinent literature, we analyze the behavior of heat current within another type of spin coupling. In Ref. [23], for instance, an XY model in a transverse field is considered (see Appendix C), for a system of four spins, in which the coupling rates are of the same order of magnitude as the frequencies of the isolated spins, $\Delta \sim h$. However, the heat baths are modeled by the phenomenological method. Figure 3 of Ref. [23] indicates that heat current first increases to a maximal value and then vanishes, with respect to the gradient of temperature (varying T_L , keeping $T_R = 0$), that is, the higher the gradient, the smaller the current, for high T_L . We show in Appendix C that such unexpected behavior is due to the use of a phenomenological approach outside its range of validity. It is worth to highlight that our formalism solves the apparent paradox in the XY model. It yields a physically sound prediction, where the current saturates at a finite value, proportional to the number of occupied quantum levels of the system, not decreasing with respect to the increase of temperature gradient (see Appendix C).

VI. OPTIMAL RECTIFICATION

Finally, asymmetric conduction of heat as a function of the temperature gradient is studied. We focus back on the system formed by two interacting spins as described via Ising model. We start in the most asymmetric scenario, where $T_L \rightarrow \infty$ and $T_R \rightarrow 0$. Then, the cycle rate simplifies to $\Gamma = -\kappa\Delta/4$ [Eq. (A7) in Appendix A], and the current to $J_L = \kappa\Delta^2/2 > 0$ [Eq. (A8) in Appendix A]. Therefore, finite conduction is established from the left to the right. On the opposite limit, $T_L \rightarrow 0$, we find that $\Gamma \rightarrow 0$, irrespective of T_R . Hence, perfect thermal isolation takes place, $J_L(T_L \rightarrow 0) = 0$, when the temperature gradient is reversed. Optimal rectification is, therefore, present in that scenario. Interestingly, the phenomenological method predicts vanishing current in both directions (see Appendix B), hence null rectification. This reinforces the disparity between the formalisms.

We give now a clear picture of the asymmetry found above. The key point resides in transition $|2\rangle \rightarrow |3\rangle$, as it involves heat exchange in the opposite sense with respect to the net heat flow. Take, for instance, the case $T_L \rightarrow 0$ (cold reservoir) and $T_R > 0$ (hot reservoir), as illustrated in Fig. 1(c). The

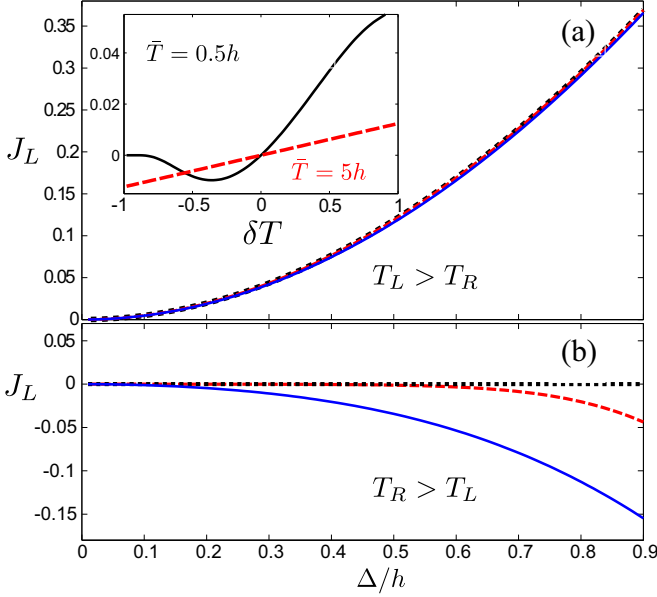


FIG. 3. (Color online) (a) Left current J_L as a function of Δ/h for (a) $k_B T_L = 10h$ and $k_B T_R = 0, 0.1h, 0.3h$, and (b) $k_B T_R = 10h$ and $k_B T_L = 0, 0.1h, 0.3h$. We used a black dotted line for $k_B T_{R(L)} = 0$, a red dashed line for $k_B T_{R(L)} = 0.1h$, and a blue solid line for $k_B T_{R(L)} = 0.3h$. When the temperature of the cold reservoir is set to absolute zero, we find optimal rectification for any value of the coupling parameter Δ . On the other hand, if the temperature of the cold reservoir is finite, it is necessary to reduce the coupling parameter to achieve optimal rectification. (Inset) Left current J_L as a function of the temperature gradient $\delta T = k_B(T_L - T_R)$ for $\Delta = 0.5h$ and $\bar{T} = 0.5h$ (black solid line), and $5h$ (red dashed line). Here $\bar{T} = k_B(T_L + T_R)/2$ denotes the average temperature. As the average temperature decreases, the curve around $\delta T = 0$ becomes asymmetric, indicating the presence of rectification.

natural path for the flow of heat is from the hot reservoir to the cold one. In order to accomplish that, heat must jump from the hot reservoir, placed on the right, into the system by flipping the right spin. In principle, two paths allow this jumping. One is the excitation from state $|1\rangle$ to $|2\rangle$ and the other is from $|3\rangle$ to $|4\rangle$. Both steps depend not only on the supply of thermal energy by the reservoir on the right, but also on the population of the state of departure. State $|1\rangle$ is the ground state, so it always has nonvanishing probability of being populated. Nevertheless, the population of $|3\rangle$ critically depends on the existence of an excitation process from state $|2\rangle$ to $|3\rangle$. We remember that $|2\rangle = |\downarrow\downarrow\rangle$ and $|3\rangle = |\uparrow\downarrow\rangle$. Thus, to pass from state $|2\rangle$ to $|3\rangle$, the system needs to gain energy by flipping the spin on the left. Only the left bath flips the left spin. If the left bath is cold, $T_L \rightarrow 0$, it is not able to provide the required energy for the left spin to flip. As a result, heat flow from the hot bath on the right to the cold one on the left is blocked precisely at transition $|2\rangle \rightarrow |3\rangle$ (formally, $\Gamma_{23}^L = \Gamma = 0$).

If the gradient is reversed so the left bath is hot, $T_L > 0$, and the right bath is cold, $T_R \rightarrow 0$, the natural path for the flow of heat also gets reversed, as illustrated in Fig. 1(b). In order to allow a finite flow of heat in the new direction, the system has to gain excitation from the left, $|1\rangle = |\uparrow\downarrow\rangle \rightarrow |4\rangle = |\uparrow\uparrow\rangle$,

and lose excitation to the right bath. It must then execute the decays $|4\rangle \rightarrow |3\rangle$ and $|2\rangle \rightarrow |1\rangle$. Again, this is only possible if an intermediate transition occurs, i.e., $|3\rangle \rightarrow |2\rangle$. This involves losing energy to the hot reservoir on the left. But that happens with finite probability per unit of time ($\Gamma_{32}^L = -\Gamma = \kappa \Delta/4 > 0$), in contrast to the absorption of heat from a cold reservoir as in the previous case.

Figure 3 proves that optimal rectification is robust to the more realistic scenario where the cold reservoir is not exactly at zero temperature. We compare $J_L(\Delta)$ in the cases $k_B T_L = 10h \gg k_B T_R = 0h, 0.1h, \text{ and } 0.3h$, in Fig. 3(a), respectively, black dotted, red dashed, and solid blue curves, and $T_L = 0h, 0.1h, \text{ and } 0.3h \ll T_R = 10h$, in Fig. 3(b), respectively, black dotted, red dashed, and solid blue curves. Perfect isolation of heat flow still holds at $k_B T_L \sim 0.1h$ ($k_B T_R = 10h$), for couplings below $\Delta \sim 0.5h$. Hence, optimal rectification can be preserved even if both reservoirs have nonzero temperature. If the temperature of the cold bath raises above $T = 0.3h/k_B$, asymmetric conduction is suddenly reduced. We can understand this result based on the previous discussion. The existence of a heat flux when $T_R > T_L$ depends on the transition $|2\rangle \rightarrow |3\rangle$. However, as the energy associated with this transition is $\omega_{32} = h - \Delta$, the left current J_L will be approximately zero if the thermal energy supplied by the left reservoir, $k_B T_L$, is much smaller than ω_{32} .

The inset of Fig. 3 illustrates the characteristic curve of the thermal diode, $J_L(\delta T)$ at constant $\bar{T} \equiv k_B(T_L + T_R)/2$, where $\delta T \equiv k_B(T_L - T_R)$. Two average temperatures are considered: $\bar{T}_{\text{low}} = 0.5h$ (black solid curve) and $\bar{T}_{\text{high}} = 5h$ (red dashed). Asymmetry is evidently guaranteed at low average temperatures, whereas it completely ceases at high average temperatures.

VII. CONCLUSIONS

We derive a master equation for a two-spin chain, within the Ising model, valid in the strong-coupling regime $\Delta \sim h$. This formalism proves necessary for correctly describing heat flow, yielding $J_L(\delta T) > 0$ at $\delta T > 0$ not only in the strong-coupling regime $\Delta \sim h$, but also in the weak-coupling limit $\Delta \ll h$. Optimal rectification of heat current is predicted in the limit $T_{L(R)} \rightarrow 0$ with $T_{R(L)} \rightarrow \infty$. An intuitive explanation of that asymmetry is given. Optimal rectification is robust with respect to nonzero low temperatures ($T \sim 0.1h/k_B$) of the cold thermal bath. The phenomenological formalism predicts no heat flow in any direction, for the same parameter values to which rectification is optimal in the strong-coupling approach. Application of this effect to practical devices should allow, for example, temperature control of quantum circuits.

A possible subsequent study is on how the size of the chain affects rectification in the ultrastrong coupling regime. For instance, one can distinguish between the role played by surface effects and by inhomogeneity on rectification, in analogy to what happens in other contexts [36]. The influence of strong coupling in quantum thermal machines is another perspective offered by this work.

ACKNOWLEDGMENTS

D.V. thanks E. Mascarenhas for fruitful discussions. T.W., M.F.C., and D.V. acknowledge financial support from CNPq, Brazil. M.F.C. acknowledges financial support from CNPq through INCT-Informação Quântica, Brazil.

APPENDIX A: HEAT CURRENT IN THE STATIONARY REGIME

In this appendix, we calculate the full expression for net transition rate Γ . This is the rate at which the cycle of the Figs. 1(b) and 1(c) runs allowing heat flow between the two reservoirs. Our calculation starts from the system of equations (8)–(11). As we have already discussed, Eqs. (8)–(11) form a linear system of equations from which one can check that all the net transitions rates $\Gamma_{ij}^{L(R)}$ involved are equal. Thus,

$$\Gamma_{41}^L = \Gamma_{12}^R = \Gamma_{23}^L = \Gamma_{34}^R \equiv \Gamma.$$

$$\Gamma = -\frac{\kappa \Delta (h^2 - \Delta^2) \sinh(\beta_R - \beta_L) \Delta}{2[(2\Delta^2 - h^2)(\sinh \beta_L \Delta + \cosh \beta_L h \sinh \beta_R \Delta) - h^2 \sinh(\beta_R - \beta_L) \Delta - \Delta h \sinh \beta_L h (1 + \cosh \beta_R \Delta)]}, \quad (\text{A5})$$

where $\beta_{L(R)} = 1/k_B T_{L(R)}$.

Now we evaluate the low temperature limits $T_L \rightarrow 0$ and $T_R \rightarrow 0$. The limit $T_L \rightarrow 0$ results in $\Gamma = 0$ which implies $J_L = 0$, that is, for low T_L and arbitrary T_R there is no heat current.

On the other side, the limit $T_R \rightarrow 0$ results in

$$\Gamma = -\frac{\kappa \Delta (h^2 - \Delta^2)}{2e^{\beta_L \Delta} [(h^2 - 2\Delta^2) \cosh \beta_L h + h \Delta \sinh \beta_L h] + 2h^2}, \quad (\text{A6})$$

which is always negative resulting $J_L > 0$. Thus, in this case, we always have heat current from the left to the right reservoir. These two cases demonstrate the optimal rectification discussed in Sec. VI.

In the limit of high temperature in the left bath, $T_L \rightarrow \infty$, and low temperature in the right one, $T_R \rightarrow 0$, the expression for Γ simplifies to

$$\Gamma = -\frac{\kappa \Delta}{4}. \quad (\text{A7})$$

This results in a heat current of

$$J_L = \frac{\kappa \Delta^2}{2}, \quad (\text{A8})$$

from the left to the right reservoir.

APPENDIX B: PHENOMENOLOGICAL APPROACH TO THE HEAT CURRENT FOR THE ISING MODEL

In the phenomenological approach, the dissipative dynamics of the Ising model is obtained by the master equation (ME),

$$\frac{d\rho}{dt} = -i[H_S, \rho] + \mathcal{L}_L^{ph}[\rho] + \mathcal{L}_R^{ph}[\rho], \quad (\text{B1})$$

This fact results in four independent equations for Γ ,

$$\Gamma = \Gamma_{41}^L = \kappa \omega_{41} [(1 + n_{\omega_{41}}^L) \rho_{44} - n_{\omega_{41}}^L \rho_{11}], \quad (\text{A1})$$

$$\Gamma = \Gamma_{12}^R = \kappa \omega_{12} [(1 + n_{\omega_{12}}^R) \rho_{11} - n_{\omega_{12}}^R \rho_{22}], \quad (\text{A2})$$

$$\Gamma = \Gamma_{23}^L = \kappa \omega_{23} [(1 + n_{\omega_{23}}^L) \rho_{22} - n_{\omega_{23}}^L \rho_{33}], \quad (\text{A3})$$

$$\Gamma = \Gamma_{34}^R = \kappa \omega_{34} [(1 + n_{\omega_{34}}^R) \rho_{33} - n_{\omega_{34}}^R \rho_{44}]. \quad (\text{A4})$$

To find Γ , we need to solve the linear system (A1)–(A4) and find the populations in the eigenstates of the Hamiltonian ρ_{ii} in terms of Γ . After that, we can use the condition $\text{Tr} \rho = 1$, that is, we sum all the expressions for ρ_{ii} and make it equal to 1 resulting in an expression for Γ which is independent of the populations ρ_{ii} . The resulting general expression for Γ in terms of the energies h and Δ and temperatures T_L and T_R is

with

$$H_S = \frac{h}{2} \sigma_z^L + \frac{\Delta}{2} \sigma_z^L \sigma_z^R, \quad (\text{B2})$$

and

$$\begin{aligned} \mathcal{L}_{L,(R)}^{ph}[\rho] = & \mathcal{J}(h) (1 + n_h^{L,(R)}) [\sigma_{L,(R)}^- \rho \sigma_{L,(R)} \\ & - \frac{1}{2} \{\rho, \sigma_{L,(R)}^+ \sigma_{L,(R)}^- \}] \\ & + \mathcal{J}(h) n_h^{L,(R)} [\sigma_{L,(R)}^+ \rho \sigma_{L,(R)} \\ & - \frac{1}{2} \{\rho, \sigma_{L,(R)}^- \sigma_{L,(R)}^+ \}], \end{aligned}$$

where

$$n_{\omega}^{L(R)} = \left[\exp \frac{\omega}{k_B T_{L(R)}} - 1 \right]^{-1}$$

is the average number of excitations in the reservoir and $\mathcal{J}(h)$ is the spectral density. The Lindblad operators $\mathcal{L}_{L,(R)}^{ph}[\rho]$ describes the dissipative effects of a single spin, whose Hamiltonian is $H = h \sigma_z^{L(R)}/2$, coupled to a bosonic thermal reservoir [35]. In other words, these operators are deduced without taking into account the interaction between the spins. Moreover, as in our case there is no magnetic field applied to the spin on the right; the Lindblad operator $\mathcal{L}_R^{ph}[\rho]$ must be calculated in the limit $h \rightarrow 0$. For an ohmic spectral density, $\mathcal{J}(h) = \kappa h$, we have $\kappa h (1 + n_h^R) \rightarrow \kappa h n_h^R \rightarrow \kappa k_B T_R$ in the limit $h \rightarrow 0$. This result shows that $\mathcal{L}_R^{ph}[\rho]$ is proportional to T_R .

Our goal now is to calculate the heat current J_L in the stationary regime for (i) $T_R \rightarrow 0$ and $T_L \neq 0$ and (ii) $T_R \neq 0$ and $T_L \rightarrow 0$. In case (i), we have $\mathcal{L}_R^{ph}[\rho] = 0$ since this operator is proportional to T_R . Therefore, as $J_R = -\text{Tr} \{ \mathcal{L}_R^{ph}[\rho_{ss}] H_S \} = 0$ and $J_L = -J_R$ [see Eq. (7) in the paper], then $J_L = 0$. This result was illustrated in Fig. 2 in the paper. To determine the

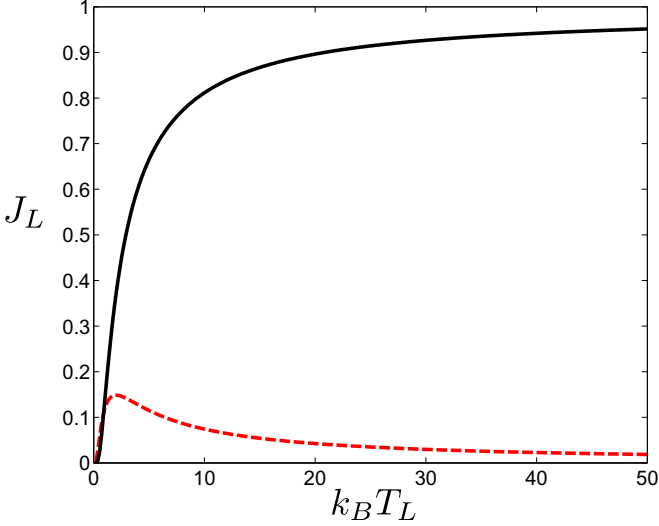


FIG. 4. (Color online) Left current J_L as a function of left bath temperature T_L for the XY model with $N = 2$ and $N = 4$. We fixed $T_R = 0$. While the left current J_L obtained through microscopic ME (black solid line) saturates at a finite value, as the left temperature T_L increases, the current obtained by the phenomenological ME (red dashed line) vanishes. The left current J_L for $N = 2$ and $N = 4$ have the same behavior.

heat current J_L in case (ii) it is necessary to determine the steady state ρ_{ss} of the ME (B1). As the steady state is diagonal in the energy eigenstates, Eq. (B1) reduces to

$$\begin{aligned}\dot{\rho}_{11} &= 0 = -h\rho_{44} + k_B T_R(\rho_{33} - \rho_{44}), \\ \dot{\rho}_{22} &= 0 = -h\rho_{33} + k_B T_R(\rho_{44} - \rho_{33}), \\ \dot{\rho}_{33} &= 0 = h\rho_{33} + k_B T_R(\rho_{11} - \rho_{22}), \\ \dot{\rho}_{44} &= 0 = h\rho_{44} + k_B T_R(\rho_{22} - \rho_{11}),\end{aligned}$$

whose solution is $\rho_{33} = \rho_{44} = 0$ and $\rho_{11} = \rho_{22} = 1/2$. So, the steady state is given by

$$\rho_{ss} = \frac{1}{2}(|1\rangle\langle 1| + |2\rangle\langle 2|) = \frac{1}{2}(|\downarrow\uparrow\rangle\langle\downarrow\uparrow| + |\downarrow\downarrow\rangle\langle\downarrow\downarrow|). \quad (\text{B3})$$

Therefore, using this steady state we have $J_L = \text{Tr}\{\mathcal{L}_L^{ph}[\rho_{ss}]H_S\} = 0$ for $T_R \neq 0$ and $T_L \rightarrow 0$.

APPENDIX C: HEAT CURRENT FOR THE XY MODEL: PHENOMENOLOGICAL VS MICROSCOPIC APPROACH

In this section we study the behavior of the heat current J_L for the XY model in the transverse field using the phenomenological ME (B1) and the microscopic ME [see Eq. (3) in the paper]. In both cases the ME dynamics was determined by numerical methods. The XY model is described by the Hamiltonian,

$$H_{xy} = \frac{\Delta}{2} \sum_{i=1}^{N-1} (\sigma_x^i \sigma_x^{i+1} + \sigma_y^i \sigma_y^{i+1}) + \frac{h}{2} \sum_{i=1}^N \sigma_z^i, \quad (\text{C1})$$

where N denotes the number of spins. Following Ref. [23], we assume $h = \Delta = 1$ (strong coupling regime).

Figure 4 shows the behavior of the left current J_L as a function of left bath temperature T_L for the XY model with $N = 2$ and $N = 4$. The temperature of the right bath is set to zero, $T_R = 0$. As previously shown in Ref. [23], as the temperature T_L increases, the heat current obtained by the phenomenological ME (red dashed line) first grows to a maximum value and then vanishes. On the other hand, using the microscopic ME we find that the heat current saturates at a finite value (black solid line). Since the excitation number of the system is conserved, the left current J_L for $N = 2$ and $N = 4$ have the same behavior.

-
- [1] S. Haroche and J.-M. Raimond, *Exploring the Quantum—Atoms, Cavities and Photons* (Oxford University Press, Oxford, 2006).
- [2] M. Brune, F. Schmidt-Kaler, A. Maali, J. Dreyer, E. Hagley, J. M. Raimond, and S. Haroche, *Phys. Rev. Lett.* **76**, 1800 (1996).
- [3] P. Maunz, T. Puppe, I. Schuster, N. Syassen, P. W. H. Pinkse, and G. Rempe, *Nature* (London) **428**, 50 (2004).
- [4] Q. A. Turchette, C. S. Wood, B. E. King, C. J. Myatt, D. Leibfried, W. M. Itano, C. Monroe, and D. J. Wineland, *Phys. Rev. Lett.* **81**, 3631 (1998).
- [5] J. Michaelis, C. Hettich, J. Mlynek, and V. Sandoghdar, *Nature* (London) **405**, 325 (2000).
- [6] J. Claudon, J. Bleuse, N. S. Malik, M. Bazin, P. Jaffrennou, N. Gregersen, C. Sauvan, P. Lalanne, and J. M. Gérard, *Nat. Photonics* **4**, 174 (2010).
- [7] A. Dousse, J. Suffczynski, A. Beveratos, O. Krebs, A. Lemaitre, I. Sagnes, J. Bloch, P. Voisin, and P. Senellart, *Nature* (London) **466**, 217 (2010).
- [8] C. Santori, D. Fattal, J. Vuckovic, Glenn S. Solomon, and Yoshihisa Yamamoto, *Nature* (London) **419**, 594 (2002).
- [9] M. Kroutvar, Y. Ducommun, D. Heiss, M. Bichler, D. Schuh, G. Abstreiter, and J. J. Finley, *Nature* (London) **432**, 81 (2004).
- [10] J. O'Brien, A. Furusawa, and J. Vuckovic, *Nat. Photonics* **3**, 687 (2009).
- [11] L. DiCarlo, M. D. Reed, L. Sun, B. R. Johnson, J. M. Chow, J. M. Gambetta, L. Frunzio, S. M. Girvin, M. H. Devoret, and R. J. Schoelkopf, *Nature* (London) **467**, 574 (2010).
- [12] A. Wallraff, D. I. Schuster, A. Blais, L. Frunzio, R.-S. Huang, J. Majer, S. Kumar, S. M. Girvin, and R. J. Schoelkopf, *Nature* (London) **431**, 162 (2004).
- [13] K. Kojima, H. F. Hofmann, S. Takeuchi, and K. Sasaki, *Phys. Rev. A* **70**, 013810 (2004).
- [14] D. E. Chang, A. S. Sorensen, E. A. Demler, and M. D. Lukin, *Nat. Phys.* **3**, 807 (2007).
- [15] A. Auffèves-Garnier, C. Simon, J.-M. Gérard, and J.-P. Poizat, *Phys. Rev. A* **75**, 053823 (2007); D. Englund, A. Faraon, I. Fushman, N. Stoltz, P. Petroff, and J. Vuckovic, *Nature* (London) **450**, 857 (2007).
- [16] D. Valente, Y. Li, J. P. Poizat, J. M. Gérard, L. C. Kwek, M. F. Santos, and A. Auffèves, *Phys. Rev. A* **86**, 022333 (2012); *New J. Phys.* **14**, 083029 (2012); E. Rephaeli and S. Fan, *Phys. Rev. Lett.* **108**, 143602 (2012).

- [17] I. Fushman, D. Englund, A. Faraon, N. Stoltz, P. Petroff, and J. Vuckovic, *Science* **320**, 769 (2008).
- [18] Z. Yu and S. Fan, *Nat. Photonics* **3**, 91 (2009).
- [19] E. Mascarenhas, D. Gerace, D. Valente, S. Montangero, A. Auffèves, and M. França Santos, *Europhys. Lett.* **106**, 54003 (2014).
- [20] J. Hwang, M. Pototschnig, R. Lettow, G. Zumofen, A. Renn, S. Gtzinger, and V. Sandoghdar, *Nature* (London) **460**, 76 (2009).
- [21] O. V. Astafiev, A. A. Abdumalikov, Jr., A. M. Zagoskin, Yu. A. Pashkin, Y. Nakamura, and J. S. Tsai, *Phys. Rev. Lett.* **104**, 183603 (2010).
- [22] E. M. Purcell, *Phys. Rev.* **69**, 681 (1946); M. O. Scully and M. S. Zubairy, *Quantum Optics* (Cambridge University Press, Cambridge, 1997).
- [23] D. Manzano, M. Tiersch, A. Asadian, and H. J. Briegel, *Phys. Rev. E* **86**, 061118 (2012).
- [24] J. J. Mendoza-Arenas, S. Al-Assam, S. R. Clark, and D. Jaksch, *J. Stat. Mech.* (2013) P07007.
- [25] J. P. Brantut, C. Grenier, J. Meineke, D. Stadler, S. Krinner, C. Kollath, T. Esslinger, and A. Georges, *Science* **342**, 713 (2013); A. Bermudez, M. Bruderer, and M. B. Plenio, *Phys. Rev. Lett.* **111**, 040601 (2013); Y. Dubi and M. Di Ventra, *Rev. Mod. Phys.* **83**, 131 (2011); R. Lopez and D. Sanchez, *Phys. Rev. B* **88**, 045129 (2013); H. Wichterich, M. J. Henrich, H. P. Breuer, J. Gemmer, and M. Michel, *Phys. Rev. E* **76**, 031115 (2007); M. Michel, O. Hess, H. Wichterich, and J. Gemmer, *Phys. Rev. B* **77**, 104303 (2008).
- [26] K. Huang and A. Rhy, *Proc. R. Soc. Lond. A* **204**, 406 (1950).
- [27] D. Valente, J. Suffczyński, T. Jakubczyk, A. Dousse, A. Lemaitre, I. Sagnes, L. Lanco, P. Voisin, A. Auffèves, and P. Senellart, *Phys. Rev. B* **89**, 041302(R) (2014).
- [28] A. Berthelot, I. Favero, G. Cassaboïs, C. Voisin, C. Delalande, Ph. Roussignol, R. Ferreira, and J. M. Gérard, *Nat. Physics* **2**, 759 (2006); V. E. Manucharyan, J. Koch, L. Glazman, and M. H. Devoret, *Science* **326**, 113 (2009).
- [29] Y. Kubo, F. R. Ong, P. Bertet, D. Vion, V. Jacques, D. Zheng, A. Dreau, J.-F. Roch, A. Auffèves, F. Jelezko, J. Wrachtrup, M. F. Barthe, P. Bergonzo, and D. Esteve, *Phys. Rev. Lett.* **105**, 140502 (2010); Y. Kubo, I. Diniz, A. Dewes, V. Jacques, A. Dreau, J.-F. Roch, A. Auffèves, D. Vion, D. Esteve, and P. Bertet, *Phys. Rev. A* **85**, 012333 (2012).
- [30] M. Terraneo, M. Peyrard, and G. Casati, *Phys. Rev. Lett.* **88**, 094302 (2002); C. W. Chang, D. Okawa, A. Majumdar, and A. Zettl, *Science* **314**, 1121 (2006); R. Scheibner, M. König, D. Reuter, A. D. Wieck, C. Gould, H. Buhmann, and L. W. Molenkamp, *New J. Phys.* **10**, 083016 (2008).
- [31] A. Fay, E. Hoskinson, F. Lecocq, L. P. Levy, F. W. J. Hekking, W. Guichard, and O. Buisson, *Phys. Rev. Lett.* **100**, 187003 (2008).
- [32] T. Niemczyk, F. Deppe, H. Huebl, E. P. Menzel, F. Hocke, M. J. Schwarz, J. J. Garcia-Ripoll, D. Zueco, T. Hammer, E. Solano, A. Marx, and R. Gross, *Nat. Phys.* **6**, 772 (2010); M. H. Devoret, S. M. Girvin, and R. J. Schoelkopf, *Annalen der Physik* **16**, 767 (2007).
- [33] T. Werlang, A. V. Dodonov, E. I. Duzzioni, and C. J. Villas-Boas, *Phys. Rev. A* **78**, 053805 (2008); F. Beaudoin, J. M. Gambetta, and A. Blais, *ibid.* **84**, 043832 (2011); A. Ridolfo, M. Leib, S. Savasta, and M. J. Hartmann, *Phys. Rev. Lett.* **109**, 193602 (2012); A. Ridolfo, S. Savasta, and M. J. Hartmann, *ibid.* **110**, 163601 (2013); R. Stassi, A. Ridolfo, O. Di Stefano, M. J. Hartmann, and S. Savasta, *ibid.* **110**, 243601 (2013).
- [34] R. Harris *et al.*, *Phys. Rev. B* **82**, 024511 (2010); K. Kim *et al.*, *New J. Phys.* **13**, 105003 (2011); J. Simmon *et al.*, *Nature* (London) **472**, 307 (2011); P. P. Orth, I. Stanic, and K. LeHur, *Phys. Rev. A* **77**, 051601(R) (2008).
- [35] H.-P. Breuer and F. Petruccione, *The Theory of Open Quantum Systems* (Oxford University Press, Oxford, 2007).
- [36] E. Pereira, *Phys. Rev. E* **83**, 031106 (2011); E. Pereira and H. C. F. Lemos, *J. Phys. A: Math. Theor.* **42**, 225006 (2009).